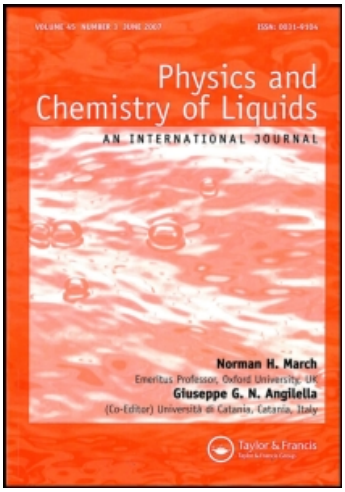

Physics and Chemistry of Liquids
Publication details, including instructions for authors and subscription information:
http://www.informaworld.com/smpp/title~content=t713646857

Temperature Effects on the Structure and Dynamics of Isomeric Pentanols by IR and Raman Spectroscopy

A. D'aprano[a]; D. I. Donato[a]; P. Migliardo[b]; F. Aliotta[c]; C. Vasi[c]
[a] Istituto di Chimica-Fisica dell'Universitá di Palermo, Palermo, Italy [b] Istituto di Fisica and CISM-GNSM del CNR, Universita di Messina, Messina, Italy [c] Istituto di Tecniche Spettroscopiche del CNR, Messina, Italy

To cite this Article D'aprano, A. , Donato, D. I. , Migliardo, P. , Aliotta, F. and Vasi, C.(1988) 'Temperature Effects on the Structure and Dynamics of Isomeric Pentanols by IR and Raman Spectroscopy', Physics and Chemistry of Liquids, 17: 4, 279 — 296
To link to this Article: DOI: 10.1080/00319108808078564
URL: http://dx.doi.org/10.1080/00319108808078564

Phys. Chem. Liq., 1988, Vol. 17, pp. 279-296
Photocopying permitted by license only

Printed in the United Kingdom

Temperature Effects on the Structure and Dynamics of Isomeric Pentanols by IR and Raman Spectroscopy

A. D'APRANO and D. I. DONATO

Istituto di Chimica-Fisica dell'Università di Palermo, Via Archirafi 26, 98123 Palermo, Italy

P. MIGLIARDO

Istituto di Fisica and CISM-GNSM del CNR, Università di Messina, Via Dei Verdi, 98100 Messina, Italy

F. ALIOTTA and C. VASI

Istituto di Tecniche Spettroscopiche del CNR, Via dei Verdi, 98100 Messina, Italy

(Received 28 May 1987)

We present IR absorption, polarized and depolarized Raman scattering data in *n*-pentanol and in 2methyl-2butanol. The measurements, performed over a wide temperature range, concern the fundamental O—H stretching vibrations. The experimental results confirm that intermolecular H-bonding effects play the main role in determining the shape and the evolution with T of the spectra. The deconvolution of the polarized Raman spectra in symmetric bands gives useful information concerning the dynamical properties of these systems. The analysis of the frequency shifts, the broadenings and the relative intensity variations with respect to the isolated O—H stretching bands confirm the existence of molecular aggregates with different spatial and/or topological conformations. The close analogy found for appropriately reduced IR absorption and depolarized Raman spectra proves that a vibrational density of states (VDOS) for both alcohols exists. These spectral features can be rationalized in terms of cooperative models recently used to interpret the vibrational dynamics of structured systems.

Key Words: Isomeric pentanols, temperature effects, IR and Raman spectroscopy.

1 INTRODUCTION

The comprehension of the hydrogen bond role in the structural and dynamical properties of hydrogenous systems, like alcohols and water,

is a problem which has been extensively studied from an experimental and a theoretical point of view.[1,2,3] It has been commonly accepted that the existence of the hydrogen bond and its highly directional intermolecular potential are the basic factors that strongly influence the chemical and the physical behaviours of these associated liquids. In particular, according to the current theories, the alcohols in the liquid phase are considered self-associated systems, whose bonding effects are triggered by a moderately strong hydrogen bond.[4,5] Although the H-bond cannot be considered as a genuine chemical bond (its energy ranges between 2 and 6 Kcal./mole and is in fact an order of magnitude lower than that of the internal O—H bond) it can originate several kinds of inter-molecular arrangements. Considering the potential energy surface of the H-bond to be originated by electrostatic, polarization, charge transfer and dispersion contributions,[3] we can expect a strict dependence of the degree of association and relative population of the local structures with both intrinsic factors (namely steric hindrance and complexity of the molecule) and external parameters (temperature and pressure).[1] Furthermore, since the mean life time of the H-bond lies in the psec. time scale, these hydrogenous liquids can be considered to be composed by "transient" structured species in dynamical equilibrium,[6,7] with time steps imposed by a continuous breaking and reforming of the bonds.

Although such dynamic aspects have recently been investigated by several Molecular Dynamics studies[8] and X-rays and Neutron diffraction experiments,[2,9] an explanation of the association phenomenon in alcohols is far from complete.

In view of the cross-link between the inherent structures, that correspond to the various local minima in the potential energy surface of the system, and the dynamical response, the vibrational spectroscopy is a powerful tool for the investigation of the different kinds of aggregates and their relative distributions.[3,4,10,11] It is a well established fact that the main information yielding vibrational dynamics in alcohols is due to the O—H stretching mode. A great number of works concerning the intramolecular O—H vibration has been reported in literature.[4,10,11,12,13] Several factors are hypothesized to contribute to the distribution of the spectra over a large frequency range (~ 1000 cm^{-1}), to the intensity and to the shape of the stretching band in such systems. The original narrow O—H band, centered at ~ 3600 cm^{-1}, as observed by IR and Raman scattering in the gas phase at high temperature, undergoes in fact strong changes[4] in the liquid phase summarized in the following: i) low wave-number shift, ii) broadening and extended spectral structure appearance, iii) variation with the

temperature of the shape, intensity and depolarization ratio in a light scattering experiment.

Although these changes, representing almost direct evidence of intermolecular O···H bonding effects, they are difficult to explain by unique theoretical model. As an example the factors that should be considered to explain the band shift effects and the potential surface shapes can be derived by quantum mechanical computations and/or anharmonic coupling of the O—H fundamental vibration with low frequency intermolecular modes, and/or intermolecular interactions. In addition, band broadening effects (for details see the extensive study performed by Bratos and coworkers[4,14]) can be rationalized in terms of anharmonic effects more or less coupled with the polarization and structural phenomenon.

Recently Raman scattering measurements on *n*-Pentanol (*n*-PeOH) and 2Methyl-2Butanol (2M—2BuOH) were performed in our laboratory.[15] The polarized spectral components were deconvoluted in symmetric bands. For the tertiary alcohol, according to previous structural studies carried out by some of us with different techniques,[16,5] an association degree higher than two was not considered. Consequently the four vibrational O—H sub-bands obtained were assigned to monomers, open dimers, and to two cyclic dimers with a different conformational arrangement. In the case of *n*-PeOH (less sterically hindered than 2M—2BuOH) the various subbands were related to monomers, open dimers and two different oligomers with an aggregation number greater than two.

In order to obtain a better understanding of the connection between the different hypothesized environments for the two alcohols studied and the vibrational dynamics, we present a detailed analysis of the polarized Raman spectra as a function of the temperature as well as a comparison between infrared absorption spectra and Raman scattering data. In our opinion, the results confirm the previous hypothesized correlation between polarized Raman bands and local structures.

We will also show that, on the basis of the cooperative character of the dynamics of these systems, a close similarity between the Raman reduced spectral density (as obtained from the anisotropic scattering) and the analogous quantity derived from the IR absorption data, exists. This allows us to apply solid state concepts[17,18] to the vibrational dynamics of associated liquids as well as to obtain significant insights into the nature of the spectral features as probed by different techniques.

2 EXPERIMENTAL PROCEDURE AND RESULTS

High-purity *n*-PeOH and 2M—2BuOH (certified grade quality products) were further purified as previously described[5] and physical impurities were removed by filtering them in a dry box. The same purified products were used to prepare the corresponding deuterated alcohols. The preparation, made in order only to deuterate the hydrogen of the O—H group, was performed according to the following procedure: 250 cc. of dry alcohol (*n*-PeOH or 2M—2BuOH) were gently refluxed in presence of a less than stoichiometric quantity of Sodium until of the latter disappeared. The Sodium alcoholate obtained was firstly evaporated under vacuum at 100°C and D_2O was then added. By distillation over Calcium hydride the middle fraction (between 115°C and 121°C for *n*-PeOD and between 95°C and 102°C for 2M—2BuOD) was recuperated. Deuterated alcohols were finally obtained from the above azeotropic mixture by crystallization. Gas-chromatographic analysis of the deuterated alcohols showed only traces of H_2O and/or D_2O. NMR spectra showed a ratio R—OH/R—OD equal to 0.75 in both alcohols. The physical impurities (such as dust particles, etc.) were also removed by filtering the alcohols in a dry box.

In the light scattering experiments the samples were sealed in optical quartz cells and were then mounted in an especially designed optical thermostat where the temperature stability, in the whole range studied, was better than 0.1°C. We used a 90° scattering geometry with a fully computerized SPEX triple monochromator using the 5145 Å line (1 Watt) of a SPECTRA PHYSICS Ar^+ laser as exciting sources. The measurements were performed in the VV and VH polarization geometries, in the temperature range between 266.2 K and 402.3 K for 2M—2BuOH and between 243.2 K and 435.6 K for *n*-PeOH. The entire experimental set-up as well as the collection and normalization of the data with the incident beam intensity was controlled on line by a DIGITAL MINC 11/23 minicomputer. Raman spectra with a mean resolution of 5 cm^{-1} were taken in the region from 2600 cm^{-1} to 3800 cm^{-1} of Stokes shift for both alcohols. As far as the infrared spectroscopy measurements are concerned, transmission spectra were recorded with a PERKIN-ELMER Mod. 983 Spectrometer with CaF_2 windows and Mylar spacers, of 10 μm of thickness for both alcohols.

The wave numbers spanned were in the range between 2600 cm^{-1} and 4000 cm^{-1} and a spectral resolution of 3 cm^{-1} was used. The variable temperature control system allowed us to perform measurements over the 278–349 K temperature range with a constancy of 1 degree.

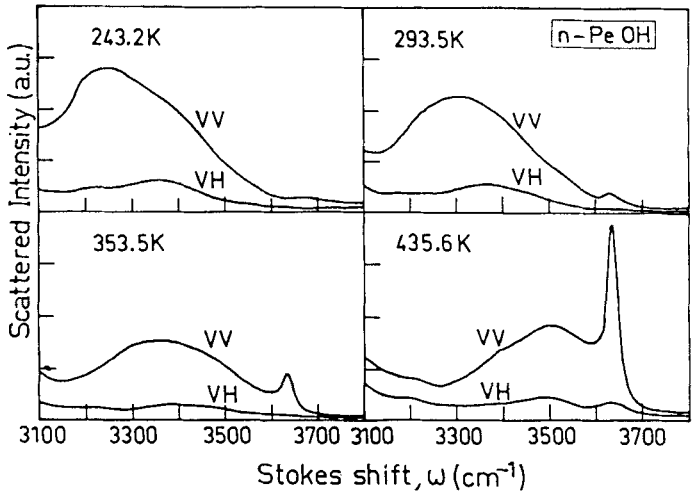

Figure 1 Polarized (VV) and depolarized (VH) Raman spectra of normal pentanol at four temperatures in the O—H stretching region.

Figures 1 and 2 represent Raman spectra at different temperatures for both the polarization geometries for *n*-PeOH and 2M—2BuOH respectively. As expected for hydrogen bond associated molecules the primitive internal O—H stretching mode is spread over a wide spectral region indicating the cooperative character of these modes. Since the

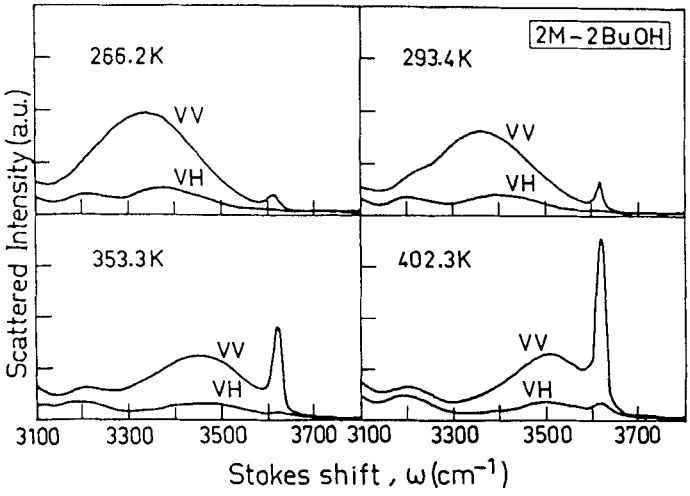

Figure 2 Polarized (VV) and depolarized (VH) O—H intramolecular spectra of 2Methyl-2Butanol at four temperatures.

Table 1 Raman spectroscopic parameters for 2Methyl-2Butanol

T (K)	ω_1 (cm^{-1})	ω_2 (cm^{-1})	ω_3 (cm^{-1})	ω_4 (cm^{-1})	Γ_1 (cm^{-1})	Γ_2 (cm^{-1})	Γ_3 (cm^{-1})	Γ_4 (cm^{-1})	I_1/I_T (%)	I_2/I_T (%)	I_3/I_T (%)	I_4/I_T (%)
266.2	3308	3360	3458	3615	74	53	42	1.0	66.4	25.3	8.2	0.1
278.2	3325	3365	3463	3616	75	53	42	1.5	64.4	26.5	8.8	0.3
293.4	3328	3407	3478	3617	77	53	42	2.5	60.0	28.9	10.4	0.7
313.1	3347	3422	3484	3617	78	54	43	3.5	54.9	30.7	12.6	1.8
333.6	3359	3442	3508	3617	80	54	43	5.0	49.7	31.6	15.2	3.5
353.3	3365	3448	3513	3621	77	55	44	6.5	36.4	34.2	21.7	7.7
367.4	3367	3450	3522	3621	73	55	45	7.5	22.2	34.9	28.6	14.3
402.3	3365	3450	3523	3623	65	56	52	9.5	8.5	23.6	43.1	24.8

Table 2 Raman spectroscopic parameters for *n*-Pentanol

T (K)	ω_1 (cm^{-1})	ω_2 (cm^{-1})	ω_3 (cm^{-1})	ω_4 (cm^{-1})	Γ_1 (cm^{-1})	Γ_2 (cm^{-1})	Γ_3 (cm^{-1})	Γ_4 (cm^{-1})	I_1/I_T (%)	I_2/I_T (%)	I_3/I_T (%)	I_4/I_T (%)
243.2	3286	3405	3480	3673	115	85	45	3	77.2	21.1	1.6	0.1
258.4	3298	3415	3484	3670	103	84	50	3	69.8	27.1	3.0	0.1
268.1	3283	3394	3480	3638	94	84	53	4	61.1	33.9	4.9	0.1
278.3	3295	3398	3480	3638	93	84	54	5	61.6	33.4	4.8	0.2
293.5	3290	3388	3480	3638	85	83	57	6	50.0	41.2	8.4	0.4
313.2	3290	3380	3480	3638	82	83	62	7	43.3	43.3	12.2	1.2
333.3	3300	3392	3480	3638	80	81	67	9	41.0	40.5	16.5	2.0
353.5	3308	3410	3500	3638	80	79	69	9	37.4	38.3	21.0	3.3
370.3	3320	3420	3519	3638	80	78	77	9	32.4	36.0	27.1	4.5
407.4	3308	3400	3525	3638	80	77	82	9	20.0	28.5	43.6	7.9
435.6	3315	3410	3525	3638	80	77	88	10	19.0	19.3	51.0	10.7

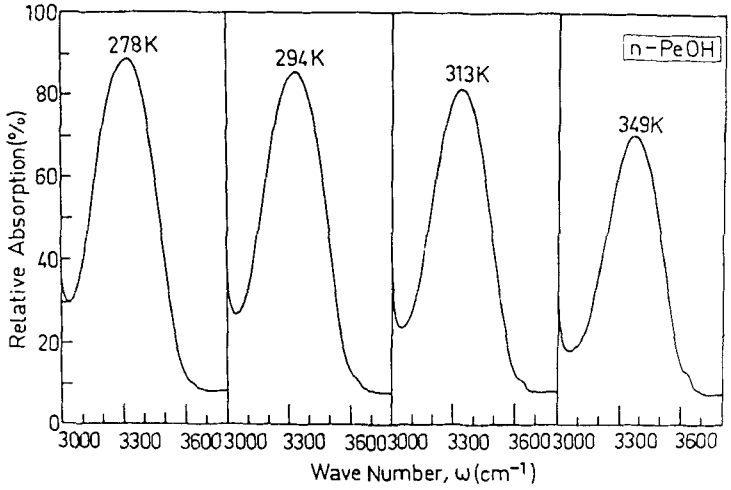

Figure 3 IR absorption spectra $(I_0 - I)/I_0$ of the O—H stretching of *n*-PeOH at four temperatures.

vibrational contribution in the VV configuration is mainly due to the isotropic portion of the spectra, we have performed a deconvolution in symmetric bands using the computer analysis previously described.[15] As referred in Ref. 15, because the C—H stretching bands overlap the O—H fundamental vibrations, we have removed the former from the spectra by evaluating it from the corresponding deuterated *n*-PeOD and 2M—2BuOD.

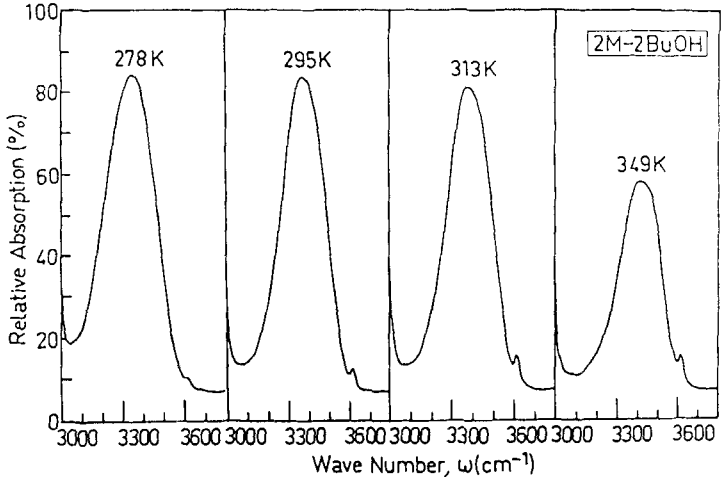

Figure 4 IR absorption spectra $(I_0 - I)/I_0$ of the O—H vibration of 2M-2BuOH at four temperatures.

Tables 1 and 2 summarize the values of center frequencies ω, widths (HWHM) Γ and percentage of areas I obtained for *n*-PeOH and 2M—2BuOH at various temperatures.

Figures 3 and 4 represent for *n*-PeOH and 2M—2BuOH respectively the relative absorption $((I_0 - I)/I_0$ at various temperatures, in the same wave numbers region examined by Raman spectroscopy. Given the connection of both IR absorption coefficient and anisotropic Raman scattering with the vibrational density of states VDOS $g(\omega)$,[18,19,20] our data have been treated without any deconvolution in order to have a direct comparison between IR and Raman spectral response. Details on this point will be extensively discussed in the next section.

3 DISCUSSION

A Polarized Raman scattering

The main purpose of our discussion is to have a better understanding of the self-associated molecular species, previously postulated in the two pentanol isomers, through a detailed analysis of the internal vibrational mode as a function of the temperature. For clarity the results will be discussed separately for *n*-PeOH and 2M—2BuOH.

n-PeOH As mentioned in Section 1, the polarized spectral contribution $I_{vv}(\omega)$ mainly reflects the isotropic coherent dynamical structure factor. On the basis of the previous results[15] the bands centered at ω_4 and ω_3 (see Table 1 of Ref. 15) have been assigned to free and/or end

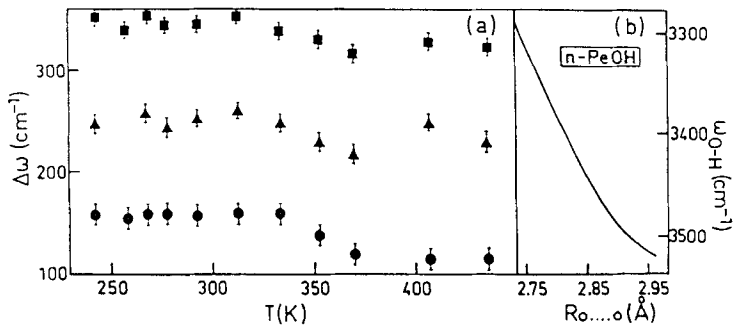

Figure 5 (a) Temperature dependence of the frequency shift $\Delta\omega = \omega_{\text{x}-\text{H}\cdots\text{O}} - \omega_{\text{O}-\text{H}}$ for the components of the polarized Raman spectra in *n*-PeOH. Squares: $\omega_4 - \omega_1$; triangles: $\omega_4 - \omega_2$; circles $\omega_4 - \omega_3$. (b) Relationship between the bond length $R_{O\cdots O}$ and the fundamental O—H on hydrogenous systems.

O—H groups and dimeric unit respectively, while the remaining bands (ω_1 and ω_2) have been assigned to oligomers with aggregation numbers greater than two. Figure 5a represents the $\Delta\omega$ shifts ($\Delta\omega = \omega_4 - \omega_i$, $i = 1, 2, 3$) as a function of temperature. As can be seen, a decreasing trend exists for all the self-associated species as T increases.

As pointed out by different authors[4,8,9] the frequency shift is strictly correlated to the variation of the potential surface minimum that reflects the change in the O···O distance. In order to find this connection, in Figure 5b the empirical correlation chart[21] between the O···O distance and the frequencies, is reported. A comparison of Figures 5a and 5b allows us to explain the following features:

a) Because higher frequency shifts are connected to more extended species, we can expect longer $R_{O...O}$ distances for dimers than for oligomers.

b) For the different n species we observe a decreasing of the frequency shift $\Delta\omega = \omega_4 - \omega_n$ ($n = 1, 2, 3$) with the increasing of the temperature. This indicates that the intermolecular $R_{O...O}$ distance becomes longer in agreement with the correlation chart indications. This behaviour can be justified by taking into account that anharmonicity and disordering effects play a major role at higher temperatures.

We next consider the band width evolution with the temperature. From an inspection of Table 1 we note that the half width associated with free or end groups are more than one order of magnitude narrower than those of the other species where hydrogen bond is present. In addition the Γ_n ($n = 1, 2, 3$) increases with the extent of the structure. Since various mechanisms contribute to the broadening of the bands,[4] and in view of the gaps in the existing theory we are forced to give only a qualitative interpretation of such a phenomenon.

As far as the temperature changes are concerned, the relatively large broadening can be rationalized by considering the overlap[4] of the molecular reorientation and anharmonicity effects. A similar increase with temperature is shown by the line width Γ_3 of the dimeric band. In our opinion, an additional factor is to be taken into account in this case: the finiteness of the mean life time of the H-bond originates in fact a fluctuation of the local environment with consequent time dependent polarization phenomena. As far as the more extended structures are concerned, the effects of the structural disorder, associated with the temperature, dominate the anharmonicity effects, so that an overall narrowing with the increasing of the temperature for the oligomer bands (Γ_1 and Γ_2) results.

It must be pointed out that (although this is outside the objective of

our study) the knowledge of the overtone bands evolution[4] could allow the separation of these two contributions.

In a first approximation the intensities of the spectral bands are connected with the scatterer populations. From this point of view the variation of the intensities shown in Figure 6 indicates that the higher oligomers, densely populated at lower temperatures, evolve as a transient species towards the simpler aggregates (monomers and dimers) as the temperature increases. As far as the I_2 behaviour is concerned the presence of the maximum can easily be explained by attributing the increase of the population on the left side as due to the transition of the higher oligomers I_1 to the lower aggregates whereas the decrease on the right side corresponds to the increase in the population of dimers and monomers.

2M—2BuOH As previously pointed out, in view of the more compact geometry of 2M—BuOH with respect to the isomer *n*-PeOH, self-associated species higher than dimers cannot be expected. The four bands obtained by the deconvolution of VV spectra have shown that, besides monomers and open dimers, two cyclic dimers (resulting by weak intermolecular hydrogen bond between C—H of C_4 methyl group with one of the oxygen lone pair orbital) also exist.

The different O···O distances observed in this case with respect to the open dimers strictly support our previous assignments.[15] In order to have a deeper understanding on this point let us consider the behaviour of $\Delta\omega_i$ as a function of the temperature, shown in Figure 7a and its correlation with the empirical distance correlation chart (Figure 7b). An inspection of the figure shows that $\Delta\omega_i$ for all the species, are temperature dependent with a decreasing of the slope as T increases.

Concerning the relative value of $\Delta\omega$ for the three different species, we observe that, while the frequency shift $\Delta\omega_3$ attributed to the open dimers corresponds to an $R_{O\cdots O}$ distance very close to the one found for the corresponding species in *n*-PeOH, for the other two species a smaller $R_{O\cdots O}$ distance is observed. This latter result can be rationalized by considering the increase in the hydrogen bond strength necessary to hold these bulkier structures. Unfortunately, in the absence of appropriate quantum-mechanical calculations, it is practically impossible to distinguish which of the two conformers (with the lone pair oxygen orbital on the same side or on the opposite side respect to the O—H bond plane) corresponds to $\Delta\omega_1$ and $\Delta\omega_2$ shifts.

Let us now consider the HWHM values reported in Table 2. As previously observed for *n*-PeOH the half widths associated with free or end groups are much smaller than those observed for the other species.

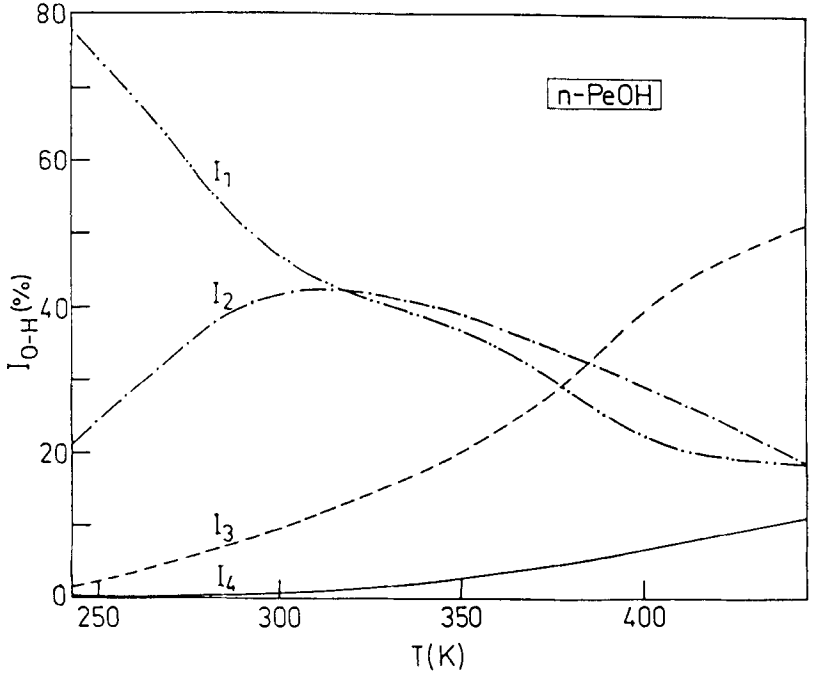

Figure 6 Temperature dependence of the integrated area I_n (n = 1, 2, 3, 4) of the O—H polarized Raman bands in n-PeOH.

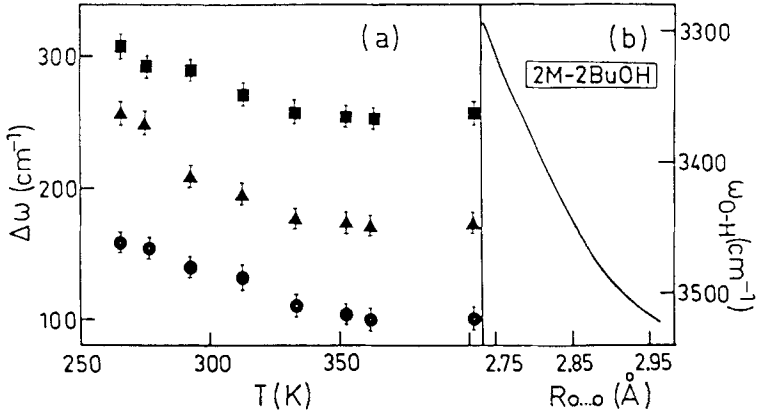

Figure 7 (a) Temperature dependence of the frequency shift $\Delta\omega = \omega_{O-H\cdots O} - \omega_{O-H}$ for the components of the polarized Raman spectra in 2M-2BuOH. Squares: $\omega_4 - \omega_1$; triangles: $\omega_4 - \omega_2$; circles $\omega_4 - \omega_3$. (b) Relationship between the bond and length $R_{O\cdots O}$ and the fundamental O—H on hydrogenous systems.

In addition a broadening of Γ_4 as T increases (imputable to similar mechanism considered for *n*-PeOH) is present. For the other three species we observe an almost temperature independent broadening of Γ. The values are also less differentiated than those obtained for *n*-PeOH probably arising from the bigger steric hindrance of the alkyl chain present in 2M—2BuOH that do not allow aggregates with coordination numbers higher than two.

In Figure 8 the evolution of the relative intensities of the various deconvoluted bands vs. T is shown. As one can see, the relative intensity associated with the unbonded O—H groups increases with T, and reach a value of 24.8% at the higher temperature examined. The integrated area I_3 associated with the open dimers shows quite a similar behaviour to that of the *n*-PeOH.

The I_1 and I_2 intensities are furthermore connected with the existence of the two cyclic conformers. Considering the behaviours of I_1 and I_2 vs. T, we can see that, while I_1 dramatically decreases as T increases, I_2 shows a wide maximum at ~ 360 K. This indicates that the population of the conformers having the smaller intermolecular O···O distance (i.e. that associated with I_1) decreases when T increases in a dynamic process in which the other species are populated.

A convincing argument for our previous choices for the assignments of the dimeric bands in 2M—2BuOH is obtained from the comparison of the evolution of the band associated with the open dimers in *n*-PeOH with the corresponding bands in 2M—2BuOH, as shown in Figure 9, where the relative intensities I_3 (Figure 9a) and the center frequency shifts $\Delta\omega_3$ (Figure 9b) for the two alcohols are plotted vs. T.

B Infrared and depolarized Raman spectra

The analysis of the Raman scattering results was performed considering that the O—H spectra are mainly induced by H-bonding effects. In other words, with the exception of the band centered at $\sim 3600\ cm^{-1}$. (due to isolated O—H groups) all the other vibrational bands are "collective types."

In the last few years it has been shown that, as in the case of disordered systems such as vitreous and amorphous materials, the structured liquids also exhibit a dynamical response successfully rationalized in terms of cooperative excitations. In particular, for molten salts like B_2O_3[22] and $ZnCl_2$[18] and $SbCl_3$[23] (in which a spatial connectivity arises from intermolecular binding effects), for concentrated electrolytic solutions[24] (in which the structural arrangement is similar to that of the corresponding hydrated crystals) and for H-bonded liquids like

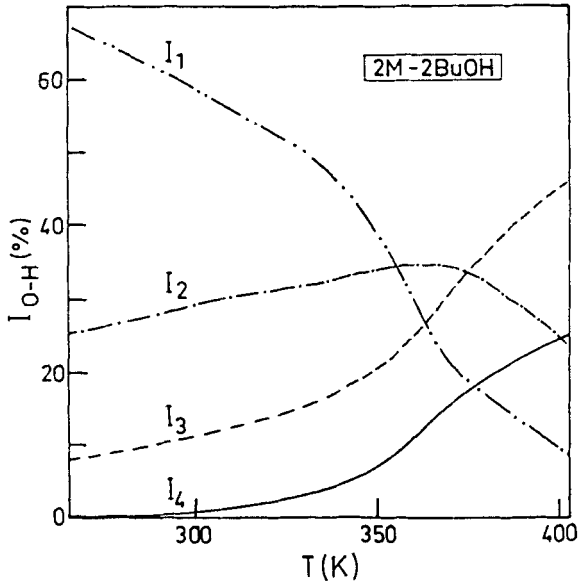

Figure 8 Temperature dependence of the integrated area I_n (n = 1, 2, 3, 4) of the O—H polarized Raman bands in 2M-2BuOH.

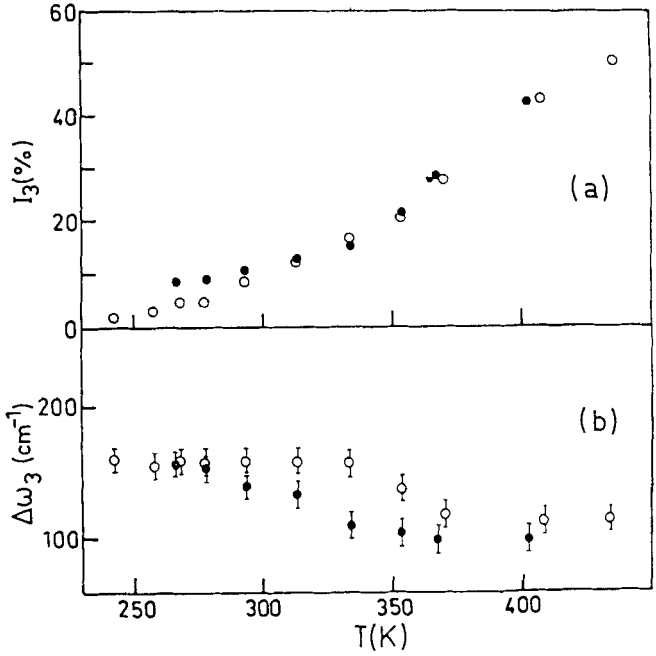

Figure 9 Temperature dependence of the intensity I_3 (a) and frequency shift $\Delta\omega_3$ (b) for the open dimeric species in n-PeOH (open circles) and 2M-2BuOH (full circles).

water,[17] the vibrational modes seem to be collective in character. In such cases, the isotropic component of the spectra can be directly connected with the eigenmodes of the system at a transferred wavevector $k \sim 10^{-4}$ Å^{-1}, whereas the anisotropic (depolarized) component $I_{anis}(\omega)$ is related to the vibrational density of states (VDOS) of the system owing to the breakdown of the translation symmetry. Under these assumptions, we have performed a suitable deconvolution in symmetric bands of the isotropic (polarized) spectra, whereas the anisotropic contributions give rise to a broader frequency spectrum interpreted in a general way as the "true" generalized frequency distribution $g(\omega)$ times a Raman electron-vibration coupling function $P(\omega)$[24]. It is worth noting the close similarity between inelastic light and inelastic neutron scattering studies. In fact, after a suitable data reduction, the coherent and incoherent inelastic neutron scattering shows features that can be related to the isotropic and anisotropic light scattering, respectively.

As far as the infrared absorption data are concerned, according to this interpretation of the vibrational dynamics, a substantially analogous data reduction can be performed. In this case, it can be shown that the IR absorption spectra give rise to the same "true" $g(\omega)$ times the transition matrix elements $D(\omega)$.

Let us write the data reduction expression for both the anisotropic Raman scattering $I_{anis}(\omega)$ and the infrared absorbance $\varepsilon_2(\omega)$. For the Raman response, the experimental $I_{anis}(\omega)$ allows us to write the Raman effective density of states $g^R_{eff}(\omega)$ by the equation[23]:

$$g^R_{eff}(\omega) = (\omega_0 - \omega)^{-4}\omega \cdot \frac{1}{n(\omega, T) + 1} \cdot I_{anis}(\omega) \tag{1}$$

where ω is the Stokes frequency shift and ω_0 is the excitation frequency, $(\omega_0 - \omega)^{-4}$ takes into account the Stokes extra-radiation factor and the dielectric fluctuation correlation factor in the quasi-harmonic approximation. In Eq. (1) the term $n(\omega, T) + 1 = [\exp(\hbar\omega/KT) - 1]^{-1} + 1$ is the Bose–Einstein population factor. In turn the $g^R_{eff}(\omega)$ is related to the true $g(\omega)$[19,20] by:

$$g^R_{eff}(\omega) \sim \sum_b P^b(\omega) \cdot g_b(\omega) \tag{2}$$

where the summation is extended to all the sub-bands b.

At the same time, it can be shown that the experimental infrared absorbance spectrum is related to the true $g(\omega)$ by the equation:

$$\omega \cdot \varepsilon_2(\omega) \sim \sum_b D^b(\omega) \cdot g_b(\omega) \tag{3}$$

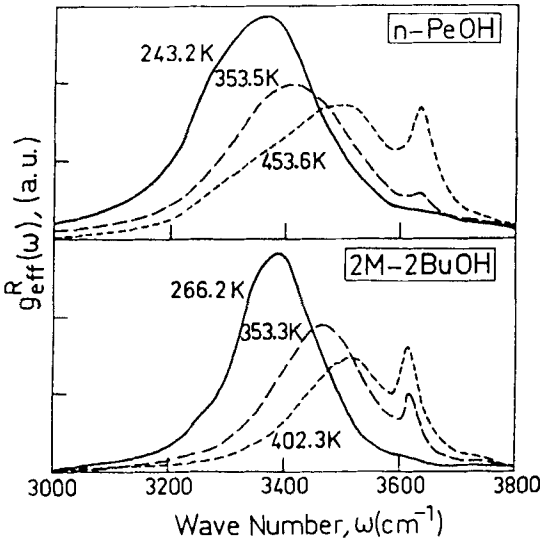

Figure 10 Temperature dependence of the Raman effective density of states for *n*-PeOH and 2M-2BuOH.

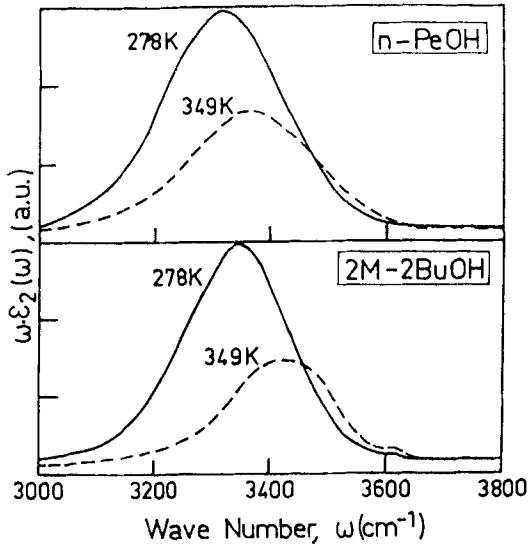

Figure 11 Infrared frequency distribution of *n*-PeOH and 2M-2BuOH as a function of *T*.

On the basis of the above models, our IR absorbance and anisotropic Raman data, suitably reduced, give for the two alcohols the quantities $g^R_{eff}(\omega)$ and $\omega \cdot \varepsilon_2(\omega)$ as a function of the temperature. The results are shown in Figures 10 and 11. In particular Figure 10 shows the Raman derived spectral distribution functions at three temperatures in the region of wave number from $3000\,cm^{-1}$ to $3800\,cm^{-1}$ for the two alcohols. These spectral densities are, as expected, broader than the isotropic components. Figure 11 shows the infrared derived spectral distribution functions at two temperatures in the region of wave numbers from $3000\,cm^{-1}$ to $3800\,cm^{-1}$. As expected these latter spectral densities are similar to the corresponding Raman ones. At this point, in order to find the quantity of interest $g(\omega)$, both the coupling coefficients (or matrix elements) $P^b(\omega)$ and $D^b(\omega)$ must be determined. Unfortunately, these quantities are practically unknown, and only recently have a few attempts of quantum mechanical calculations for the force constants determination been made.[19,20]

As an alternative procedure we can estimate the $g(\omega) \sim \sum_b g_b(\omega)$ from an inelastic incoherent neutron scattering experiment (IINS) and then obtain direct information about the ω-dependence of the coupling coefficients, without using theoretical calculations. Comparison between the IR and Raman and Neutron response for this purpose exists in literature only in a few cases.[20,24] Unfortunately, since IINS data have not been carried out so far in our system, it is not possible to know $P_b(\omega)$ and $D_b(\omega)$ or to follow the temperature evolution of these quantities. However we can note that the IR and Raman spectral patterns observed for the two alcohols show some similarity in the shapes. This evidence suggests that we can assume that $g^R_{eff}(\omega)$ and $\omega \cdot \varepsilon_2(\omega)$ to consist of a linear combination of sub-bands VDOS $g_b(\omega)$ times different coupling coefficients "ω-independent" over the width of each b band.

According to the above hypothesis, we could say that our spectral densities mimic the "true" VDOS. In our opinion, the answer to this problem can be definitely obtained by an appropriate IINS experiment.

4 CONCLUDING REMARKS

In this paper we have presented an analysis of the high-frequency vibrational dynamics of the two *n*-PeOH and 2M—2BuOH isomeric alcohols. The O—H stretching region was investigated in a very large temperature range from the normal to the superheated liquid state by the use of both IR absorption and Raman scattering techniques. The

results allow us also to draw the following conclusions:

i) the polarized (= isotropic) spectra unambiguously show the H-bonding effects through the strong influence of the symmetric sub-bands parameters by the temperature. The connection between the local structure (i.e. association phenomenon) and vibrational bands is discussed in terms of a cooperative model for the light scattering. The existence of monomers and dimeric unities (open and cyclic) are confirmed for the sterically hindered 2M—2BuOH. On the contrary monomers, dimers and oligomers give rise to vibrational bands with a frequency shift that increases with the spatial extent. The relative intensity of the bands are strongly T dependent. These circumstances were connected to the existence in both alcohols of a hierarchy of structures with relative population that varies with T by means of a microscopic dynamic process. We have also observed a common trend for the two systems: lower temperature tends to promote topologically more extended structures.

ii) The frequency contributions to the anisotropic Raman spectra were directly connected with the IR absorbance spectra. Both Raman and IR responses give information on the vibrational density of the states (VDOS) that is convoluted with the transition matrix elements.

Our results conclusively confirm that the O—H fundamental vibrational in associated alcohols can be understood in terms of H-bond imposed binding effects.

Acknowledgement

We are deeply indebted to Prof. L. Pellerito of the University of Palermo, Chem. Dept., for his assistance and useful discussion during the IR measurements. Thanks are also extended to Dr. L. Hobbins for helpful suggestions and revision of the English text.

References

1. For a comprehensive review on the Hydrogen bonds theories and experiments the reader is referred to: *The Hydrogen bond*, P. Schuster, G. Zundel and C. Sandorfy, Vol. I, II, III, North-Holland (1976).
2. D. G. Montague and J. C. Dore, *Mol. Phys.*, **57**, 1035 (1986) and references therein.
3. P. A. Kollman and L. C. Allen, *Chem. Rev.*, **72**, 283 (1972).
4. D. Hadzi and S. Bratos, *Vibrational spectroscopy of the Hydrogen bond* in The hydrogen bond, P. Schuster, G. Zundel and C. Sandorfy, Vol. II, North-Holland, p. 565 (1976).
5. A. D'Aprano, D. I. Donato, G. D'Arrigo, D. Bartolini, M. Cassettari and G. Salvetti, *Mol. Phys.*, **55**, 475 (1985).
6. G. Fytas and Th. Dorfmuller, *J. Chem. Phys.*, **75**, 5232 (1981).
7. H. G. Hertz and M. D. Zeidler, *Nuclear Magnetic Relaxation in Hydrogen bonded liquids* in *The Hydrogen bond*, P. Schuster, G. Zundel and C. Sandorfy, Vol. III, North-Holland, p. 1026 (1976).

8. M. L. Jorgensen, *J. Am. Chem. Soc.*, **103**, 335 (1981) and references therein.
9. I. Olovsson and P. G. Jonsson, *X-ray and Neutron diffraction studies of Hydrogen bonded systems* in The Hydrogen bond, P. Schuster, G. Zundel and C. Sandorfy, Vol. II, North-Holland, p. 393 (1976).
10. W. A. P. Luck, *The angular dependence of Hydrogen bond interactions* in *The Hydrogen bond*, P. Schuster, G. Zundel and C. Sandorfy, Vol. II, North-Holland, p. 527 (1976).
11. D. Maillard, C. Perchard and J. P. Perchard, *J. Raman Spectrosc.*, **7**, 178 (1978) and references therein.
12. L. Wilson, R. Bicca de Alencastro and C. Landorfu, *Can. J. Chem.*, **63**, 40 (1984).
13. C. Bouderon, J. Peron and C. Sandorfy, *J. Chem. Phys.*, **76**, 864 (1972).
14. S. Bratos, *Infrared and Raman Study of Vibrational Relaxation in Liquids* in *Vibrational Spectroscopy of Molecular Liquids and Solids*, S. Bratos and F. Pick, Vol. 56-B, Plenum NY, p. 43 (1980).
15. A. D'Aprano, D. I. Donato, P. Migliardo, F. Aliotta and C. Vasi, *Mol. Phys.*, **58**, 213 (1986).
16. A. D'Aprano, D. I. Donato and V. Agrigento, *J. Solution Chem.*, **10**, 673 (1981).
17. F. Aliotta, C. Vasi, G. Maisano, D. Majolino, F. Mallamace and P. Migliardo, *J. Chem. Phys.*, **84**, 4731 (1986).
18. M. L. Caccciola, S. Magazu', P. Migliardo, F. Aliotta and C. Vasi, *Solid State Comm.*, **57**, 513 (1986).
19. G. Zerbi, *Vibrational Spectroscopy of Very Large Molecules* in *Adv. in IR and Raman Spectr.*, R. J. H. Clark and R. E. Hester, Vol. 11, Wiley, pp. 330–334 (1984).
20. F. L. Galeener, A. J. Leadbetter and M. W. Stringfellow, *Phys. Rev. B*, **27**, 1052 (1983).
21. A. Novak, *Struct. and Bond*, **17**, 177 (1974).
22. R. Shuker, R. and R. Gammon, *J. Chem. Phys.*, **55**, 4784 (1971).
23. F. Aliotta, G. Maisano, P. Migliardo, C. Vasi, F. Wanderlingh, R. Triolo and G. P. Smith, *J. Chem. Phys.*, **76**, 3987 (1982).
24. G. Maisano, P. Migliardo, M. P. Fontana, M. C. Bellisent-Funel and A. J. Dianoux, *J. Phys. C*, **18**, 1115 (1985).